Induction of Apoptosis by Green Synthesized Gold Nanoparticles Through Activation of Caspase-3 and 9 in Human Cervical Cancer Cells

Javad Baharara [1*], Tayebe Ramezani [2], Adeleh Divsalar [3], Marzieh Mousavi [1], and Arefeh Seyedarabi [4]

1. Animal Developmental Biology, Research Center for Animal Development Applied Biology and Department of Biology, Mashhad Branch, Islamic Azad University, Mashhad, Iran
2. Department of Animal Biology, Faculty of Biological Sciences, Kharazmi University, Tehran, Iran
3. Department of Cell and Molecular Biology, Faculty of Biological Sciences, Kharazmi University, Tehran, Iran
4. Institute of Biochemistry and Biophysics, University of Tehran, Tehran, Iran

* Corresponding author:
Javad Baharara, Ph.D., Animal Developmental Biology, Research Center for Animal Development Applied Biology and Department of Biology, Mashhad Branch, Islamic Azad University, Mashhad, Iran
Tel: +98 511 8437092
Fax: +98 511 8437092
E-mail:
baharara@mshdiau.ac.ir

Abstract

Background: Gold Nanoparticles (GNPs) are used in imaging and molecular diagnostic applications. As the development of a novel approach in the green synthesis of metal nanoparticles is of great importance and a necessity, a simple and safe method for the synthesis of GNPs using plant extracts of *Zataria multiflora* leaves was applied in this study and the results on GNPs' anticancer activity against HeLa cells were reported.

Methods: The GNPs were characterized by UV-visible spectroscopy, FTIR, TEM, DLS and Zeta-potential measurements. In addition, the cellular up-take of nanoparticles was investigated using Dark Field Microscopy (DFM). Induction of apoptosis by high dose of GNPs in HeLa cells was assessed by MTT assay, Acridin orange, DAPI staining, Annexin V/PI double-labeling flow cytometry and caspase activity assay.

Results: UV-visible spectroscopy results showed a surface plasmon resonance band for GNPs at 530 *nm*. FTIR results demonstrated an interaction between plant extract and nanoparticles. TEM images revealed different shapes for GNPs and DLS results indicated that the GNPs range in size from 10 to 42 *nm*. The Zeta potential values of the synthesized GNPs were between 30 to 50 *Mev*, indicating the formation of stable particles. As evidenced by MTT assay, GNPs inhibit proliferation of HeLa cells in dose-dependent GNPs and cytotoxicity of GNPs in Bone Marrow Mesenchymal Stem Cell (BMSCs) was lower than cancerous cells. At nontoxic concentrations, the cellular up-take of the nanoparticles took place. Acridin orange and DAPI staining showed morphological changes in the cell's nucleus due to apoptosis. Finally, caspase activity assay demonstrated HeLa cell's apoptosis through caspase activation.

Conclusion: The results showed that GNPs have the ability to induce apoptosis in HeLa cells.

Introduction

The unique physicochemical properties of nanoparticles made them promising substrates for the development of applications which cover a vast and diverse array of areas including engineering, biology, physics and chemistry [1]. Gold Nanoparticles (GNPs) are amongst one of the most extensively studied areas since the first report of gold colloids by Faraday dates back to more than 100 years ago [2]. GNPs can be used to label DNA or protein for detection of biological targets with enhanced sensitivity. They are primarily used in imaging, and molecular diagnostic applications [3]. Biocompatibility, toxicity and the ability to penetrate cells are three certain factors that will determine the application of a nano product in medicine [4]. However, most of the synthetic systems recorded to date rely heavily on toxic reducing agents like sodium borohydride and organic solvents such as N, N-dimethylformamide, which lead to serious environmental issues for vast synthesis. Hence, there is a growing need to develop environmentally safe nanoparticle synthesis processes that do not apply toxic chemicals. Therefore, the biosynthesis technology has received increasing attention because of a cleaner and simpler biosynthesis. The use of environmentally benign materials like plant ex-

tracts, fungi and bacteria for the synthesis of nanoparticles, such as GNPs, has increased and attracted attention in recent years [5].

Zataria multiflora (*Z. multiflora*) referred as "Avishen-e- Shirazi" (in Persian), is a famous traditional Iranian medicine. *Z. multiflora* is a member of the Lamiaceae family and used in traditional folk remedies for its antiseptic, analgesic and carminative properties [6,7]. The main constituents of this plant are phenolic compounds such as carvacrol, thymol and eugenol that have antibacterial effects [8]. This plant grows in the south of Iran, Pakistan, India, and Afghanistan. The leaves of *Z. multiflora* were used in the food industry as a preservative and also for its flavor [6].

Since cancer remains one of the world's most devastating diseases and current cancer treatments include surgical intervention, chemotherapeutic drugs and radiation, which often also kill healthy cells and cause toxicity to the patient [9], the new therapeutic methods should have fewer side effects for cancer patients. Gold nanoparticles are widely investigated for biological applications and medical purposes due to their unique optical properties and electrochemical stability [10]. Therefore, in the present study, gold nanoparticles were synthesized using medical plant of *Z. multiflora* extract, and then the apoptotic effects of capped GNPs with medical plant extract against cervical carcinoma HeLa cells were studied. In fact, gold nanoparticles also act as a carrier for *Z. multiflora* extract. This plant extract was also reported to have antioxidant and anticancer effects [8].

Materials and Methods

Chemicals

HAuCl$_4^-$·3H2O, RPMI, 3-(4,5-dimethylthiazol-2-yl)-2,5-diphenyltetrazolium bromide, yellow tetrazole (MTT), penicillin-streptomycin, DAPI (4_,6-diamidino-2-phenylindole, dihydrochloride), ethidium bromide and Acridine orange were all purchased from Sigma-Aldrich. Annexin-V-FITC was purchased from abcam. *Z. multiflora* leaves were collected from local natural sources (Khorasan province, Mashhad). HeLa cells were obtained from the National Cell Bank of Iran (NCBI)-Pasteur Institute of Iran and BMSCs were obtained from rat bone marrow. All solutions were prepared with double distilled water.

Plant extract preparation

Z. multiflora leaves were collected from Shiraz, Iran in May. The identity of the plant material was confirmed by a plant taxonomist from the Herbarium Division of the Ferdowsi University with the voucher specimen number 34516. The leaves were then washed thoroughly 3 times with double distilled water, and air-dried in the shade at room temperature for a week, powdered in a mixer. Following this step, 5 *g* of the powdered leaves was added to 100 *ml* of sterile distilled water in a 500 *ml* Erlenmeyer flask and boiled for 5 *min*. The extract was then filtered through a What-

man filter (paper No.1). The solution was then stored at 4°*C* for further use.

Synthesis of gold nanoparticles and characterization techniques

In a typical experiment, the leave extract (0.1 up to 1 *ml*) was added to 10 *ml* of 1 *mM* chloroauric acid (HAuCl$_4$) aqueous solution. Change in the color of the solution indicates the formation of the nanoparticles. This process was carried out at room temperature and at pH=7.

After the addition of the gold salt solution to the plant extract, the color of the solution was changed from colorless to ruby red indicating the formation of GNPs. UV-visible absorption spectra of AgNPs were measured at the wavelength of 300-700 *nm* using a spectrophotometer (Biotake, Epuch, US). The average size of the nanoparticles was determined using DLS (Cordovan, Vaso particle, France). The sample with the best UV-visible peak was selected for the DLS study. DLS was used to determine the size distribution profile of GNPs at 25 *C* using 0.894 cp for the viscosity of the medium, a fixed angle of 90 *C* for the Avalanche Photo Diode (APD) detector and a wavelength of 657 *nm* for the 50 *mW* laser. Stability of the nanoparticles was determined using Zeta potential analysis. Zeta-potentials of GNPs in water were evaluated using CAD (Zeta compact zeta sizer, France). Samples were sonicated for 5 *min* before measurements in order to ensure that the particles were well dispersed and the dispersion was homogeneous. The morphology and size of the GNPs were investigated by TEM images (CM 30, Philips, Windhaven, and T Netherlands). For imaging, thin films of the samples were prepared on a carbon coated copper grid by just dropping a very small amount of the samples on the grid and allowing it to dry in a desiccator at room temperature. Grids were viewed using a transmission electron microscopy. FTIR for plant leave extract and GNPs was obtained in the range of 4,000 to 400 cm^{-1} with a Perkin Elmer spectrophotometer paragon 1000. In order to remove any free biomass residue or unbound extract from the surfaces of the GNPs, the GNPs were repeatedly washed with distilled water. Subsequently, the product was centrifuged at 9000 *rpm* for 10 *min* and dried. The powdered GNPs were mixed with KBr powder and FTIR spectra were obtained in the range of 4,000 to 400 cm^{-1}.

Cell culture

The human tumor cell line (HeLa) and BMSCs were selected for the cytotoxicity study of GNPs. Cells were grown in RPMI. This medium was supplemented with 10% FBS and 1% penicillin-streptomycin (Sigma) at 37 *C* under a 5% CO$_2$/ 95% air atmosphere.

In vitro cytotoxicity study and cellular uptake

The *in vitro* cytotoxicity of GNPs in HeLa cells and BMSCs (as normal cells) was studied using the MTT assay. The cleavage and the conversion of the soluble

yellowish MTT (sigma) to the insoluble purple form-azan by active mitochondrial dehydrogenase of living cells has been used for the measurement of cell proliferation. Harvested cells were seeded into a 24-well plate (1×10^5 *cell/ml*) with different amounts of GNPs (0-400 *µg/ml*) for 48 *hr*. At the end of the incubations, 20 *µl* of MTT solution (5 *mg/ml* in PBS) was added to each well containing fresh and cultured medium. The insoluble formazan produced was dissolved in a solution containing 1 *ml* of isopropanol (Merck) and left for 4 *hr* at room temperature in dark conditions. Finally, the Optical Density (OD) was read against a blank reagent using a well scanning spectrophotometer (Bio-tek Epoch, US) at 570 *nm*. The viability of the cells was calculated using the equation below:

Viability of treatment cells (%)=($A_{treated}/A_{control}$)×100

where $A_{treated}$ and $A_{control}$ are the absorbance of the treated and untreated cells, respectively [4].

Dark field microscopy (DFM)

DFM was used to determine the cellular uptake of GNPs. For this reason, the HeLa cells were treated with 80 *µg/ml* GNPs, based on the MTT results, and after a 48 *hr* treatment, the cells were analyzed by dark field microscopy (Biomed, Korea).

Acridine orange and ethidium bromide staining

A dye mixture in equal ratios of acridine orange and ethidium bromide was prepared and mixed with the cell suspension solution and placed on a clean microscopic cover slip. After incubation for approximately 2-3 *min*, cells were visualized under a fluorescence microscope at 40× magnification via an especial filter at 510-590 *nm*. The percentage of apoptotic cells was calculated using the formula below:

$$\%\text{apoptotic cells} = \frac{\text{Total number of apoptotic cells}}{\text{Total number of normal and apoptotic cells}} \times 100$$

DAPI staining

The treated HeLa cells were fixed with a solution of methanol: acetic acid (3:1, *v/v*) prior to washing with PBS. The washed cells were then dyed with DAPI (4, 6-diamidino-2-phenylindole, dihydrochloride) in the dark. Stained images were captured using a fluorescent microscope with an appropriate filter (Biomed, Korea).

Determination of apoptotic and necrotic cells

The amount of the externalization of phosphatidyl-serine (PS) from HeLa cell surfaces was determined by the Annexin-V-FITC staining kit (Abcam, Germany) according to the manufacturer's instructions. The cells were treated with 100 *µg/ml* for 24 and 48 *hr* and then harvested and centrifuged at 200×*g* for 5 *min*. Subsequently, the cell pellet was resuspended in binding buffer. Following that step, 5 *µl* of Annexin- V-FITC labeling solution and 5 *µl* of PI solution were added to the mixture, and incubated for 5 *min* at 25 *°C* and then analyzed with a flow cytometer (Bd, UK).

Caspase activity assay

A quantitative enzymatic activity assay was carried out according to the instructions of the manufacturer for the colorimetric assay kit (Abcam, Germany). After treatment with GNPs (100 *µg/ml* for 24 *hr*), cells were washed, collected, lysed, centrifuged, and analyzed for total protein by the Bradford assay. Samples containing 200 *µg* of total protein were assayed for caspase-3/9 activity with DEVD-pNA as a caspase-3-specific substrate. Absorbance was measured at 405 *nm* in a plate reader.

Statistical analysis

Statistical evaluation of the data was performed using a one-way analysis of variance (ANOVA) and a Tukey test was used for multiple comparisons as a posttest with the help of SPSS software. Results were shown as mean±SD and p<0.05 was calculated as the minimum level of significance.

Results

Synthesis of gold nanoparticles and characterization techniques

The present study reports the green synthesis of GNPs by the reduction of aqueous $HAuCl_4$ using the *Z. multiflora* leaf extract. The formation of the GNPs could be detected by the change in color of the reactive mixture of gold solution and plant extract. Solutions of colloidal GNPs have a distinctive red color, characteristic of GNP formation due to the excitation of surface plasmon vibrations in GNPs. In the case of the mixture ratio of 10 *ml* of $HAuCl_4$ and 1 *ml* of leaf extract (10:1 *v/v*), changes in the color of the reaction mixture started within 30 *min* at room temperature. Higher ratios of the mixture, up to 10 *ml* of plant extract and 10 *ml* of $HAuCl_4$, did not lead to the formation of nanoparticles. At lower ratios of the mixture, a weak color change was observed. No significant color change was seen in either the control or the sample which only contained the pure aqueous $HAuCl_4$ solution. Results have shown that increasing the amounts of leaf extract leads to a decreased efficiency in nanoparticle synthesis. The color for the extract and $AuCl_4$ combined solution changed to light ruby red within 30 *min* at room temperature and later changed to dark ruby red during the incubation period (Figure 1). It is well known that the small GNPs exhibit only one Surface Plasmon Resonance (SPR) absorption band. The SPR bands centered between 500-600 *nm* indicate the formation of GNPs in
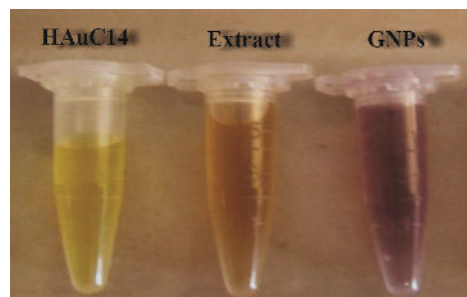

Figure 1. Visual appearance of color change in vials containing the *Zataria multiflora* leaves extract, AuHCl₄ solution and GNPs at room temperature after 4 *hr* of mixing with AuHcl₄.
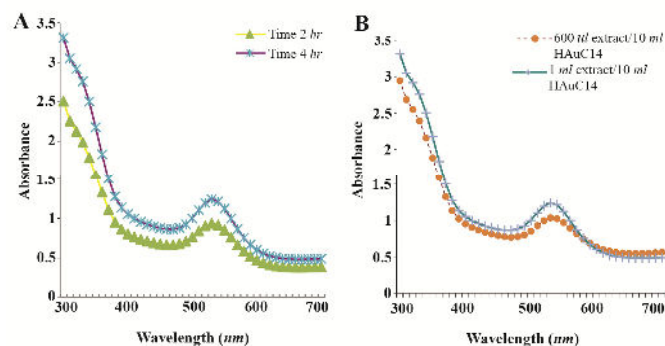
Figure 2. UV-Visible spectra of AgNPs at different time intervals. A) UV-Visible spectra of GNPs at different extract concentrations; B) the sharp peak in 530 *nm* appeared in UV-Visible spectrum.

Figure 4. Particle size distribution of synthesized GNPs. The range was from 10-80 *nm* and average size of nanoparticles was 21.13 *nm*.

Figure 5. Zeta-potential of synthesized GNPs appeared negative between -20 to -50.

solution. Therefore, the reduction of gold ions to GNPs was analyzed using UV-visible spectrophotometer in the wavelength range of 300-700 *nm* at regular time intervals. The maximum absorbance of GNPs was seen at 540 *nm* (Figure 2A), and the surface plasmon band for GNPs solution remained close to 540 *nm* throughout the reaction period indicating that the particles were dispersed in the aqueous solution, with no evidence for aggregation. It is notable that the best peak was seen in the ratio of 10 *ml* of AuCl$_4$ and 1 *ml* of plant extract (Figure 2B). The use of greater volumes (up to 10 *ml*) of extract led to the deposition of GNPs and a color change in the solution, which is unfavored. Additionally, the GNPs did not represent any peak in the wavelength range of 300-700 *nm*. It was also observed that the intensity of the surface plasmon bands increased as the reaction time progressed from 0-4 *hr* and then remained at a near to constant intensity, indicating the completion of the reaction process (Figure 2A). The nanoparticles were seen to be well-dispersed without the need for any physical and/or chemical capping agents. The synthesized GNPs from leaf extract were observed to be very stable in solution, even after 1 month of synthesis. According to these results, a mixture of 10:0.7 (*v/v* ratio) of HAuCl$_4$ and leaf extract was selected for further analysis. A sucrose density gradient separation was also performed to improve the monodispersity of GNPs. Figure 3A shows the typical
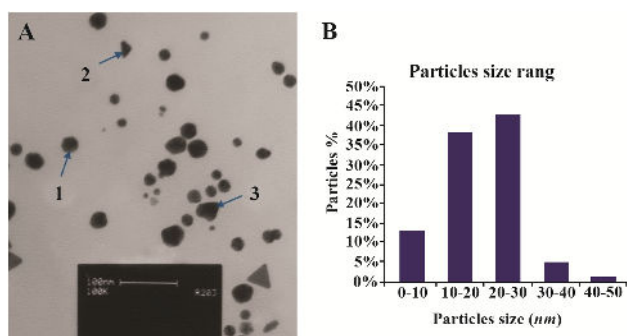

Figure 3. A) Transmission electron microscope images of the green synthesized GNPs; B) Particle size distribution histogram of GNPs determined from TEM image analyzed by the Image J software.
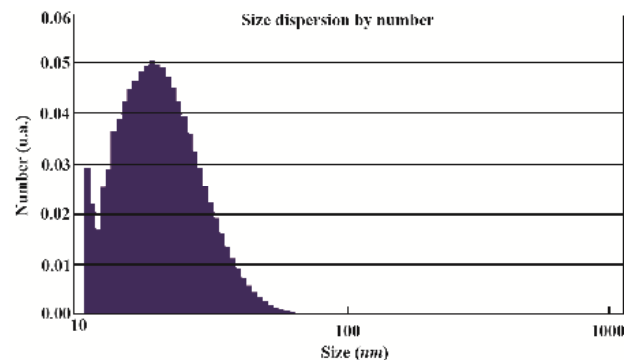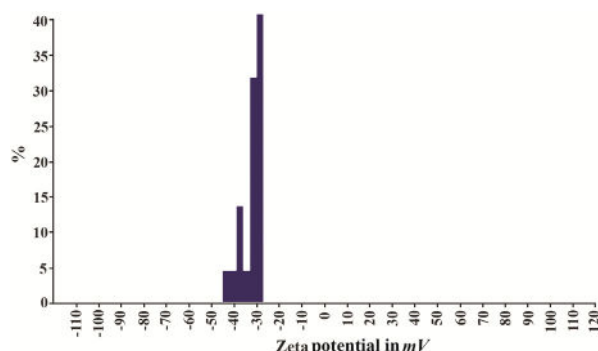
bright-field TEM micrograph of the synthesized GNPs. As shown in figure 3A, GNPs are of different shapes; pentagons (arrow marked 1), larger propensity of triangular nanoparticles (arrow marked 2) and some of undefined shapes (arrow marked 3). Figure 3B shows the size distribution of nanoparticles centered on 10-50 *nm*, therefore, giving an average diameter of 20.52 *nm* for the nanoparticles. Additionally, the TEM image shows that all nanoparticles tend to be well separated from each other without the formation of aggregates. DLS results showed that the average diameter of nanoparticles were 21.13 *nm* and indeed agree with the results obtained from TEM analysis (with a diameter of 20.52 *nm*) (Figure 4). As taken together, the data showed that the GNPs were small, uniform in size, stable and without any obvious aggregation. The Zeta sizer was used to measure the electrophoretic mobility of each nanoparticle sample. Complex Zeta potential is a parameter which is used in the study of the surface charges and stability of nanoparticles. Surface charges can greatly influence the particle size distribution and the cellular uptake of nanoparticles. In natural conditions (pH close to 7.2), the Zeta potential of the synthesized GNPs was equal to -30 to -50 *mV* (Figure 5). It could be concluded that GNPs have a negative Zeta potential and the particles are fairly stable due to their electrostatic repulsion (as a rule of thumb, ±30 *mV* is the required Zeta potential to keep dispersion charge stabilized).
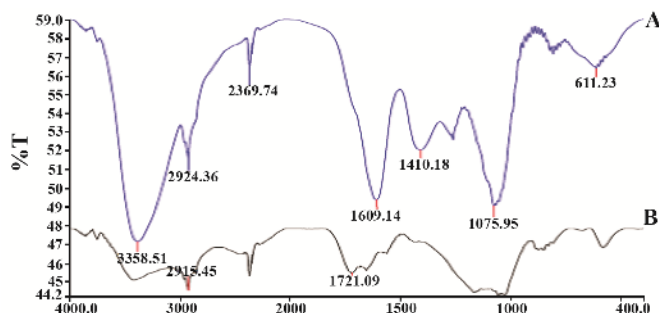
Figure 6. FTIR absorption spectra of dried *Zataria multiflora* leaf extract before bio reduction; A) and after complete bio reduction; B) at room temperature. These spectra were similar and plant extract covered GNPs.
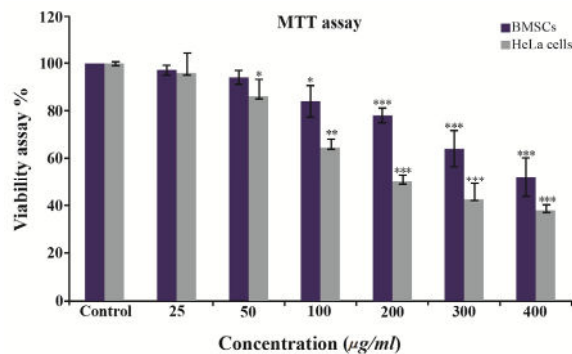

Figure 7. Effects of different concentrations of GNPs on HeLa cells compared to BMSCs viability after 48 *hr* of treatment. The significant ($p<0.05$) decrease in cell viability was observed in a dose dependent manner. The values are shown as mean±SD.

FTIR measurements were carried out to identify candidate biomolecules responsible for efficient stabilization and capping of GNPs synthesized using *Z. multiflora* leaves. Figure 6 shows the FTIR spectrum of synthesized GNPs in this study. The representative spectra of nanoparticles exhibit absorption peaks located at 3388, 2928, 1721, 1075 and 611 cm^{-1} (Figure 6). The broad band contour which appears in the range of 3000-3400 cm^{-1} is the summation of intermolecular associations of hydrogen bonds related to $-NH_2$ and -OH groups in the protein molecules. The peaks at 2922 and 2852 cm^{-1} confirm the presence of the $-CH_3$ (alkanes) groups. The absorption peak at around 1077 cm^{-1} is attributed to the stretching vibrations of -C=O (ester) groups and the amount of 1721 cm^{-1} can be attributed to the C=O (ketone and aldehyde) groups. The peak at 605 cm^{-1} confirms the presence of the C-S stretch in the samples analyzed. The various functional groups mentioned above are mainly derived from *Z. multiflora*'s water soluble components. Therefore, it can be assumed that different water soluble compounds such as alkanoids and flavonoids act as capping ligands for the synthesis of GNPs.

Cytotoxicity study

The potential toxicity of the synthesized GNPs against HeLa carcinoma cells has been examined. The HeLa cells were treated with different concentrations (0-400 *µg/ml*) of nanoparticles for 48 *hr* and then MTT assay was used to measure mitochondrial activity in viable cells. As it is shown in figure 7, reduction in cell viability by ~50% (inhibitory concentration=IC_{50}) in comparison with the control was achieved at a dose of 100 *µg/ml* of GNPs, while the greatest number of cells were killed at 400 *µg/ml* of GNPs. However, cytotoxicity of GNPs in bone marrow was lower than Hela cells IC50 of GNPs in BMSCs which was 300 *µg/ml* (Figure 7).

Dark field microscopy study

In this study, DFM was used to determinate the GNPs uptake into HeLa cells. In DFM, the GNP$_S$ on the cell surface scatter yellow light due to the enhanced SRP in the visible region after 48 *hr*. The concentration
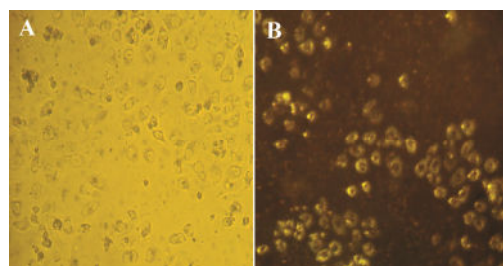

Figure 8. Bright field image of HeLa cancer cells incubated with GNPs. A) Dark-field image of a live cell after treatment (~48 *hr*) with GNPs in cancer cells; B) Cell surface scatters yellow light due to the GNPs uptake in the visible region.

of GNPs (80 *µg/ml*) used in this experiment was according to the MTT assay, which was below that of the IC_{50} value. The results showed that the nanoparticle uptake by the cells may be due to the plant material that covers the surface of the particles (Figure 8). HeLa cells which uptake nanoparticles scatter yellow light due to SRP of GNPs.

DAPI staining results

The next specific aim was to determine whether the cell viability inhibitory effect of GNPs is associated with induction of cell apoptosis. For cells treated with GNPs (0, 100 and 400 *µg/ml*) for 48 *hr*, DAPI staining assay revealed that the GNPs caused condensed nuclei and apoptotic bodies in a dose-dependent manner in HeLa cells (Figure 9).

Acridine orange results

Using a fluorescence microscope, Acridine orange staining showed that normal cells appear uniformly green whereas early apoptotic cell debris was yellow or yellowish green. Acridine orange can be used in con-
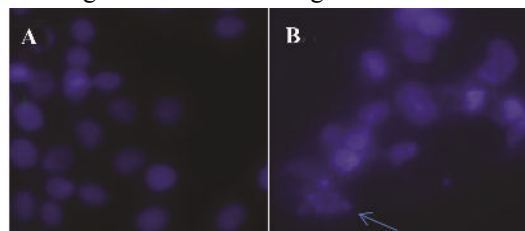

Figure 9. DAPI stained image of HeLa cells after treatment with GNPs. Choromatin fragmentation is shown with arrow.

junction with ethidium bromide to differentiate between viable, apoptotic and necrotic cells. Figure 10 shows images of control HeLa cells as well as necrotic and apoptotic cells after Acridine orange/ethidium bromide staining. Figure 10A shows the control, which did not receive any treatment. The arrows show live cells (green) and figure 10B indicates treated cells with 100 $\mu g/ml$ GNPs in late apoptotic stage (dead=orange) with condensation and chromatin clumping. Figure 10C shows that 400 $\mu g/ml$ of GNPs leads to the death of all of the cells (red).

Flow cytometer study

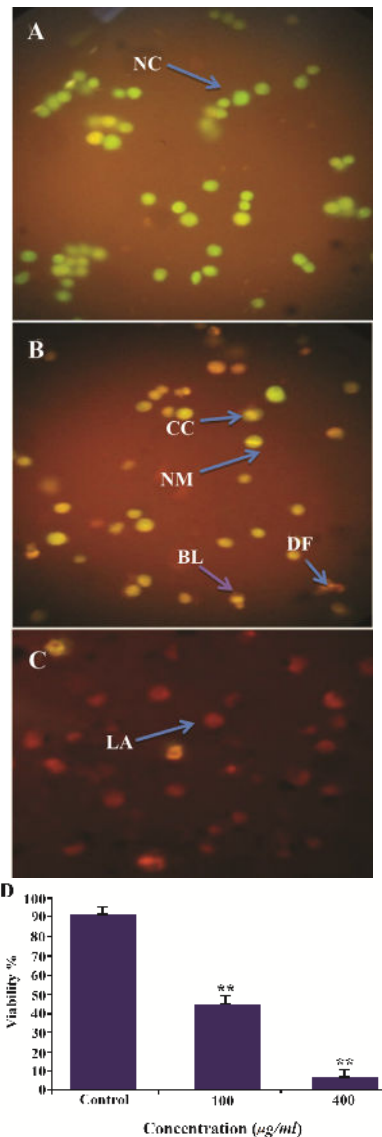Apoptosis was assessed using dual Annexin-V and PI staining kit. The proportion of cells in the lower-right quadrants, which corresponds to apoptotic cells (Annexin-V positive) increased to 23.2 and 26.4% after treating the HeLa cells with 100 $\mu g/ml$ of GNPs for 24 and 48 hr, respectively. The proportion of cells in upper and right quadrants of late apoptosis (Annexin-V positive and PI positive) increased to 7.7 and 46.2 after treating the HeLa cells with 100 and 400 $\mu g/ml$ of GNPs, respectively. These results are all hallmarks of apoptotic cell death and demonstrate the ability of GNPs to induce apoptosis in HeLa cells in a time dependant manner (Figure 11).

Caspase assay results
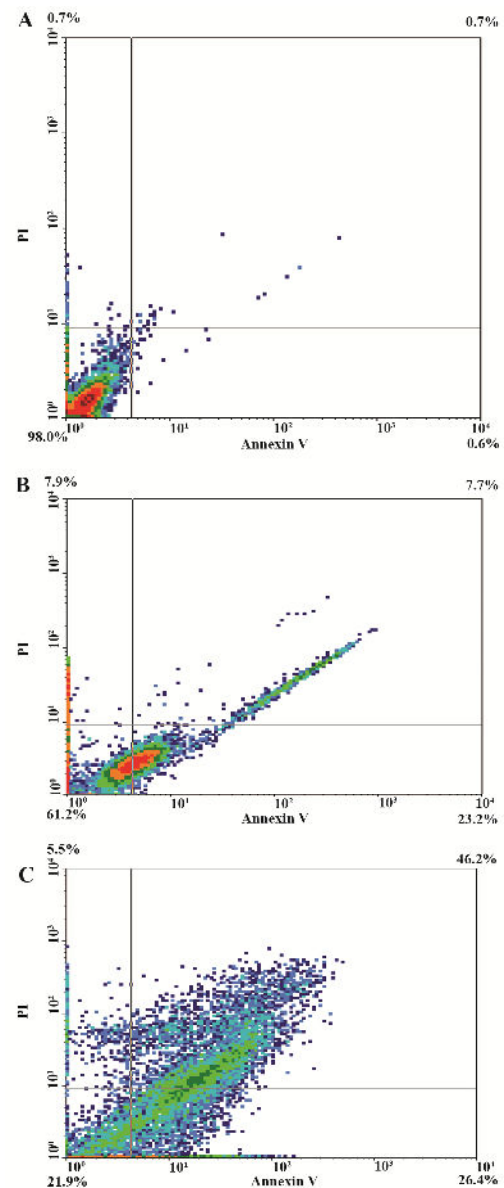
In this experimental study, caspase activation was

Figure 10. Comparison of EB/AO method for HeLa suspension cells. HeLa cells were treated with A) 0, B) 100 $\mu g/ml$ and C) 400 $\mu g/ml$ of GNPs for induction of apoptosis. Representative micrographs showing quantification of cells viability after 48 hr of treatment with 0, 100 and 400 $\mu g/ml$ of GNPs D). The cells were introduced as normal cells (NC), early apoptotic cells (EA), late apoptotic (LA) after 48 hr of treatment showing membrane blebbing (BL), chromatin condensation (CC), blebbing and nuclear margination (MN), DNA fragmentation (DF) and apoptotic body formation after 48 hr of treatment using arrows. The values are shown as mean±SD.


Figure 11. Dot plots of PI versus Annexin V staining followed by flow cytometry analyses for Hela cells at density of 10^6 $cell/ml$, based on GNPs induced externalisation of phosphatidylserin. Figures from A-C represent controls of Hela cells without treatment (A) and Hela cells treated with 100 $\mu g/ml$ (=IC$_{50}$ value) of GNPs after 24 and 48 hr (B and C, respectively).

Table 1. Flow cytometric analysis of HeLa cells treated with various concentrations of GNPs after different incubation times

Cell condition	Cells (%)		
	Control	100 $\mu g/ml$ (24 hr)	100 $\mu g/ml$ (48 hr)
Viable cells	98	61.2	21.9
Early apoptosis	0.6	23.2	26.4
Late apoptosis/necrosis	0.7	7.7	46.2
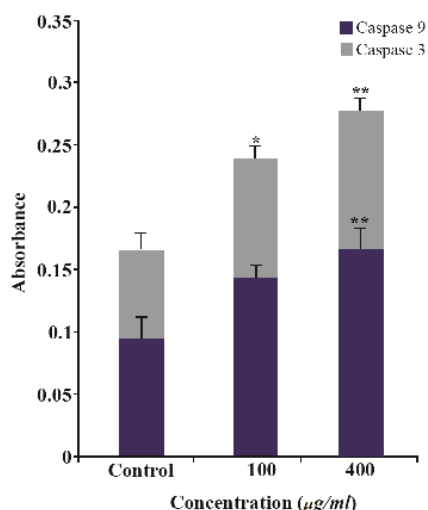
Figure 12. The activity of cellular caspase-3/9 was assayed as described in Materials and Methods. Significant differences (p>0.05) in caspase-3 and caspase-9 activity were found between the treated and control groups.

evaluated in cells treated with 100 $\mu g/ml$ of GNPs for 24 hr. Colorimetric assay of caspase-3/9 activity showed that the caspase activity in cells treated with GNPs increased significantly (p>0.05) in comparison to untreated groups. This assay indicated that BV promoted the caspase-3/9 activation in HeLa cells. The activation of caspase-3/9 during GNPs induces apoptosis of HeLa cells through caspase activiation (Table 1), (Figure 12).

Discussion

One-step green synthesis of GNPs is presented using the biodegradable *Z. multiflora* extract at room temperature, at neutral pH and without the use of external factors such as shaking. This method is simple, economical, nontoxic and efficient comparing chemical methods. The maximum absorbance of GNPs was seen at 530 *nm* which is similar to the maximum absorbance wavelength reported by Chueh *et al* [4] and Geetha *et al* [11]. Both groups used a green approach for the synthesis of GNPs distinguished with a sharp peak around 540-560 *nm* [12]. TEM image showed that the synthesized GNPs have various morphologies. He *et al* used chitosan chains for the synthesis of GNPs by a "green" method and their TEM images showed that their nanoparticles had different shapes and the size of their GNPs ranged between 10 and 50 *nm* [13]. In addition, GNPs synthesized using honey showed polymorpho-

logy which is in agreement with our results [14]. The variety in shape can be due to various herbal ingredients which can give nanoparticles a unique shape. The diameter of the GNPs was 21 *nm* in average, as shown by DLS. The flavonoid, terpenoid and protein constituents which were presented in *Z. multiflora* extract are the surface active molecules stabilizing the nanoparticles. As the evidence from measurement of Zeta potential showed, these GNPs were stable. Although the exact mechanism for the formation of GNPs is not understood, however, based on our data and other published results, the following points can be outlined. The *Z. multiflora* extract is primarily composed of carvacrol and thymol as main phenolic compounds and p-cymene as the main non-phenolic compound, respectively [15]. The active constituents of *Z. multiflora* are thymol and carvacrol giving rise to a variety of beneficial functions including antioxidant, antifungal and antinociceptive activities [16]. The antioxidant activity of phenolic compounds is due to their high tendency to chelate metals. Phenols possess hydroxyl and carboxyl groups and are able to bind to heavy metals. In addition, other reports have shown that proteins can bind to nanoparticles through free amine groups and, therefore, the stabilization of GNPs by proteins is a possibility. Therefore, it can be concluded that biological molecules could be involved in both functions of formation and stabilization of GNPs in the aqueous medium [17]. GNPs can be utilized in Photo Thermal Therapy (PTT). For example, Xiaohua Huang *et al* demonstrated that the laser power threshold for the photo thermal destruction of cells after the NP$_S$ treatment is found to be 20 times lower than that required to destroy the cells in the normal PTT, that is, without the use of NP$_S$ [18]. NPs may have the potential to improve local regional control and shorten the period needed for PTT, which may help minimize PTT side effects. According to previous reports, GNPs can act as a drug delivery system such that GNPs can bind drugs after surface modification or by ionic bonding, physical adsorption, or covalent bonding. They have the benefit of stability, high tissue permeability and small size [19]. For example, GNPs conjugated with methotrexate are efficient transporters. In this study, the FTIR spectroscopic results confirm that some various functional groups on the surface of GNPs can be used for binding various factors including protein, RNA, DNA and drugs for medical and drug delivery applications. Overall, the up-take of nanoparticles at nontoxic concentrations seems appropriate and it can be concluded that GNPs can be used for various purposes in the field of gene delivery, drug delivery and other therapy approaches such as PTT, without the need for any additional surface modifications. Most studies have used GNPs at low concentrations. Cytotoxic effect of GNPs was also assessed.

The present study shows that high doses of GNPs is cytotoxic for HeLa cells as it reduces cell viability in a concentration dependent manner; however, GNPs have

toxic effect on BMSC cells only in higher doses. More-over, a high dosage of GNPs seem to induce HeLa cell death via apoptosis that was demonstrated by results from the DAPI and Acridine orange staining and Annexin V/PI study. Mytych *et al* have assessed the cytotoxic effect of GNPs on different mammalian cell lines, including that of PK-15 (porcine kidney), Vero (African green monkey kidney), NIH3T3 (mouse embryonic fibroblast) and MRC5 (human normal lung fibroblast) cells.

They reported that GNPs induce a concentration-dependent suppression of growth in all tested cell lines, although there were different levels of inhibition among cell lines [20]. Also Bhowmik *et al* introduced a simple biosynthetic method using flower extract of *Couroupita guianensis* to synthesize GNPs and explored the anti-leukemic cancer activity of HL-60 using the synthesized GNPs. Their results indicate that the proliferation of HL-60 cells due to gold nanoparticle treatment effects were dose dependent [21].

Conclusion

These results confirmed our findings which show that the GNPs can inhibit the cell proliferation in a dose dependent manner and GNPs could induce apoptosis in HeLa cells through caspase activation. Therefore, GNPs not only have the potential for use, either by local application or via intravenous routes as a carrier, also they can be used to induce apoptosis in cancer cells with high doses. In the future, the GNPs alone, or conjugated with specified antibody or anti-cancer drugs, may be applied for the treatment of cervical cancer or other cancers which may overcome adverse effects associated with the chemotherapy and traditional radiation methods.

Acknowledgement

Conflict of Interest

The authors declare no conflict of interest.

References

1. Kanipandian N, Kannan S, Ramesh R, Subramanian P, Thirumurugan R. Characterization, antioxidant and cytotoxicity evaluation of green synthesized silver nanoparticles using Cleistanthus collinus extract as surface modifier. Mater Res Bull 2014;49:494-502.

2. Liu X, Atwater M, Wang J, Huo Q. Extinction coefficient of gold nanoparticles with different sizes and different capping ligands. Colloids Surf B Biointerfaces 2007;58(1):3-7.

3. Abdelhalim MAK, Mady MM, Ghannam MM. Physical properties of different gold nanoparticles: Ultraviolet-Visible and fluorescence measurements. J Nanomed Nanotechnol 2012;3(03):2-5.

4. Chueh PJ, Liang RY, Lee YH, Zeng ZM, Chuang SM. Differential cytotoxic effects of gold nanoparticles in different mammalian cell lines. J Hazard Mater 2014;264: 303-312.

5. Haratifar EAD, Shahverdi HR, Shakibaie M, Mollazadeh Moghaddam K, Amini M, Montazeri H, et al. Semi-biosynthesis of magnetite-gold composite nanoparticles using an ethanol extract of eucalyptus camaldulensis and study of the surface chemistry. J Nanomater 2009;2009: 1-5.

6. Motevasel M, Okhovat MA, Zomorodian K, Farshad S. A study of the effect of Zataria multiflora extract on methicillin resistant staphylococcus aureus. Jundishapur J Microbiol 2013;6(5).

7. Shokri H, Asadi F, Bahonar AR, Khosravi AR. The role of Zataria multiflora essence (Iranian herb) on innate immunity of animal model. Iran J Immunol 2006;3(4):164-168.

8. Yahyaraeyat R, Khosravi AR, Shahbazzadeh D, Khalaj V. The potential effects of Zataria multiflora Boiss essential oil on growth, aflatoxin production and transcription of aflatoxin biosynthesis pathway genes of toxigenic Aspergillus parasiticus. Braz J Microbiol 2013;44(2): 643-649.

9. Pulit J, Banach M, Kowalski Z. Nanosilver-making difficult decisions. Ecol Chem Eng S 2011;18(2):185-196.

10. Gericke M, Pinches A. Microbial production of gold nanoparticles. Gold Bull 2006;39(1):22-28.

11. Geetha R, Ashokkumar T, Tamilselvan S, Govindaraju K, Sadiq M, Singaravelu G. Green synthesis of gold nanoparticles and their anticancer activity. Cancer Nanotechnol 2013;4(4-5):91-98.

12. Lan MY, Hsu YB, Hsu CH, Ho CY, Lin JC, Lee SW. Induction of apoptosis by high-dose gold nanoparticles in nasopharyngeal carcinoma cells. Auris Nasus Larynx 2013;40(6):563-568.

13. He C, Hu Y, Yin L, Tang C, Yin C. Effects of particle size and surface charge on cellular uptake and biodistribution of polymeric nanoparticles. Biomaterials 2010;31 (13):3657-3666.

14. Alkilany AM, Murphy CJ. Toxicity and cellular uptake of gold nanoparticles: what we have learned so far? J Nanopart Res 2010;12(7):2313-2333.

15. Huang X, Qian W, El-Sayed IH, El-Sayed MA. The potential use of the enhanced nonlinear properties of gold nanospheres in photothermal cancer therapy. Lasers Surg Med 2007;39(9):747-753.

16. Ying TH, Yang SF, Tsai SJ, Hsieh SC, Huang YC, Bau DT, et al. Fisetin induces apoptosis in human cervical cancer HeLa cells through ERK1/2-mediated activation of caspase-8-/caspase-3-dependent pathway. Arch Toxicol 2012;86(2):263-273.

17. Klekotko M, Matczyszyn K, Siednienko J, Olesiak-Banska J, Pawlik K, Samoc M. Bio-mediated synthesis, characterization and cytotoxicity of gold nanoparticles. Phys Chem Chem Phys 2015;17(43):29014-29019.

18. Huang X, Jain PK, El-Sayed IH, El-Sayed MA. Determination of the minimum temperature required for selective photothermal destruction of cancer cells with the use

of immunotargeted gold nanoparticles. Photochem Photobiol 2006;82(2):412-417.

19. Hitchman A, Smith GH, Ju-Nam Y, Sterling M, Lead JR. The effect of environmentally relevant conditions on PVP stabilised gold nanoparticles. Chemosphere 2013;90 (2):410-416.

20. Mytych J, Lewinska A, Zebrowski J, Wnuk M. Gold nanoparticles promote oxidant-mediated activation of NF-κB and 53BP1 recruitment-based adaptive response in human astrocytes. Biomed Res Int 2015;2015:304575.

21. Bhowmik T, Saha PP, Dasgupta A, Gomes A. Antileukemic potential of PEGylated gold nanoparticle conjugated with protein toxin (NKCT1) isolated from Indian cobra (Naja kaouthia) venom. Cancer Nanotechnol 2013;4(1-3):39-55.